



Research Article

Dihydromyricetin Alleviates Nonalcoholic Fatty Liver Disease and Its Associated Metabolic Syndrome by Inhibiting Endoplasmic Reticulum Stress in LDLR^{-/-} Mice Fed with a High-Fat and High-Fructose Diet

Lin Liu ¹, Quan Shen,^{2,3} Yan Wang,⁴ Hong Li,⁵ and Jingshan Zhao ^{1,2,3}

¹Department of Biochemistry and Molecular Biology, College of Basic Medicine, Hebei University of Chinese Medicine, Shijiazhuang, Hebei 050200, China

²Traditional Chinese Medicine Processing Technology Innovation Center of Hebei Province, Shijiazhuang, Hebei 050200, China

³College of Pharmacy, Hebei University of Chinese Medicine, Shijiazhuang, Hebei 050200, China

⁴Department of Medical Nursing, College of Nursing, Hebei University of Chinese Medicine, Shijiazhuang, Hebei 050200, China

⁵College of Science, Shijiazhuang Engineering Vocational College, Shijiazhuang, Hebei 050200, China

Correspondence should be addressed to Jingshan Zhao; zhaojingshan@hebcm.edu.cn

Received 5 April 2023; Revised 16 June 2023; Accepted 24 July 2023; Published 8 August 2023

Academic Editor: Fares El Sayed Mohammed Ali

Copyright © 2023 Lin Liu et al. This is an open access article distributed under the Creative Commons Attribution License, which permits unrestricted use, distribution, and reproduction in any medium, provided the original work is properly cited.

Nonalcoholic fatty liver disease (NAFLD) is a chronic liver disease. Previous studies have shown that dihydromyricetin (DHM) is beneficial for NAFLD. However, whether DHM alleviates NAFLD by inhibiting liver endoplasmic reticulum (ER) stress remains unknown. Thus, this study aimed to identify the potential roles and mechanisms of DHM. Twenty-four male low-density lipoprotein receptor (LDLR^{-/-}) knockout mice aged 8 weeks were randomly divided into normal control, control, and DHM groups. Normal control mice were fed a normal diet (ND), and the last two groups of mice were fed a high-fat and high-fructose diet (HFD) for 12 weeks, treated with or without DHM. DHM alleviated diet-induced hyperlipidemia as early as 4 weeks after and until the end of HFD feeding. HFD increased insulin resistance, and the opposite was observed in the DHM group. Compared to the control group, the body weight of the mice and adipocyte size and weight of the retroperitoneal and epididymal fat were remarkably reduced in the DHM group. The expression of genes related to lipid metabolism, such as *Acox1* and *Cpt1α*, was significantly upregulated. Moreover, *Mttp* was downregulated in the two fat sites in the DHM group. DHM alleviated diet-induced lipid deposition in the liver and decreased liver triglyceride and total cholesterol content. DHM improved liver function by inhibiting ER stress, alleviating atherogenesis, and promoting vascular remodeling. In conclusion, dihydromyricetin improved NAFLD and related insulin resistance, hyperlipidemia, and atherogenesis by inhibiting liver ER stress in HFD-fed LDLR^{-/-} mice.

1. Introduction

Nonalcoholic fatty liver disease (NAFLD) is a chronic liver disease characterized by excessive deposition of lipids in hepatocytes, excluding alcohol and other damaging factors, and it is closely related to insulin resistance, hyperlipidemia, and obesity [1]. NAFLD can be categorized into simple fatty liver (SFL) disease, nonalcoholic steatohepatitis (NASH), and cirrhosis [2]. Moreover, NASH can lead to cirrhosis and liver cancer [3]. With the

global trend of obesity and related metabolic disorders, NAFLD has become a leading cause of chronic or end-stage liver disease in developed countries and rich areas of Asia [4]. The prevalence of NAFLD in the general adult population is 13 to 32%, among which 12 to 30% are NASH; cirrhosis in 10 years is up to 25% [5].

In addition to directly causing liver cirrhosis and hepatocellular carcinoma, NAFLD/NASH can contribute to the occurrence and development of type 2 diabetes and atherosclerosis (As) [6]. Malignant tumors, As, and

cirrhosis are essential factors that affect the quality of life and life expectancy of patients with NASH [6, 7]. Therefore, NASH is a new challenge in contemporary medicine, and effective prevention and therapy are urgently needed.

For patients with NASH, changing their lifestyle or taking medications is beneficial. Although anti-hyperlipidemic drugs such as statins and fibrates are widely used in treating NASH, toxicity and side effects (such as hepatic dysfunction and rhabdomyolysis) have restricted the use of these drugs [8]. Therefore, researchers are investigating the use of natural medicines to treat NASH and its associated metabolic syndromes. Dihydromyricetin (DHM) is a type of flavonoid isolated from Chinese traditional medicine, such as *Ampelopsis grosedentata*, *Vitis vinifera* L., *Ginkgo biloba* L., *Prunus amygdalus Batsch*, and *Myrica cerifera* L. [9]. In China, it has been used to treat cough, pain, pyretic fever, jaundice, and hepatitis for hundreds of years. Recently, many other potential therapeutic effects (such as ameliorating NASH-associated hyperlipidemia, insulin resistance, diabetes, As, and hepatocellular carcinoma) have been explored [10, 11]. Liu et al. demonstrated that DHM could decrease plasma low-density lipoprotein (LDL) levels and alleviate As by preventing oxidative stress, inhibiting endothelial cell injury, and forming macrophage foam cells [12]. Furthermore, recent animal studies have shown that DHM alleviates NAFLD in hamsters by regulating multiple metabolic pathways [13]. In addition, DHM can alleviate insulin resistance by inhibiting inflammation through the phospholipase C-CaMKK-AMPK signaling pathway or by upregulating insulin receptor substrate-1 tyrosine phosphorylation [11, 14].

Excessive endoplasmic reticulum (ER) stress can affect tumor cells proliferation. A few studies have explored the effects of DHM on ER stress inhibition for the prevention and treatment of cancers [15]. In addition, ER stress aggravates NAFLD/NASH and related metabolic disorders. However, whether DHM alleviates NAFLD-related fatty liver disease, insulin resistance, and As by inhibiting ER stress in the liver has not yet been studied.

To elucidate this, we used a mouse model of NAFLD/NASH-associated metabolic disorders using high-fat and high-fructose (HFD) diet-fed LDL receptor knockout (LDLR^{-/-}) mice to evaluate the effect of DHM on plasma lipids, fatty liver, insulin sensitivity, and As and to investigate its possible mechanism. We observed that suppressing liver ER stress using DHM could alleviate NAFLD/NASH and related hyperlipidemia, insulin resistance, adipose tissue expansion, and atherogenesis.

2. Materials and Methods

2.1. Materials. DHM (CAS: 27200-12-0) was purchased from Jiangsu Enming Bioengineering Technology Co. Ltd., with a 98% purity confirmed by using high-performance liquid chromatography. DHM was dissolved in a 0.5% sodium carboxymethyl cellulose (CMC-Na, Sigma-Aldrich) aqueous solution to a final concentration of 20 mg/mL.

2.2. Animals, Diets, and Experimental Designs. Twenty-four male LDLR^{-/-} mice aged 4 weeks were purchased from Beijing Vital River Laboratory Animal Technology Co., Ltd. All animals were maintained on a 12:12-h light-dark cycle and fed *ad libitum* with a normal diet (ND) or a high-fat and high-fructose diet (HFD) (20% fat, 0.5% cholesterol, and 35% fructose). All animals were fed a normal diet for 4 weeks. The mice were then challenged with ND or HFD for 12 weeks, and their body weight were recorded weekly. The mice were randomly divided into three groups of eight mice each: normal control (ND), control (HFD), and DHM (HFD + DHM) groups. The control and DHM groups' animals were fed on HFD, and the normal control group's mice were fed on ND. DHM was dissolved in a suspension using 0.5% CMC-Na. The DHM group intragastrically received 250 mg/kg body weight of DHM daily [16], and the other two groups were intragastrically administered the same volume of 0.5% CMC-Na after being fed on ND or HFD. The food intake was recorded weekly. At the end of the HFD period, all mice were anesthetized with 80 mg/kg pentobarbital sodium (Sigma-Aldrich). Tissues and thoracic aortas were harvested. Tissues for western blot and real-time quantitative PCR (qPCR) were stored at -80°C, while those for morphological detection were soaked in paraformaldehyde until analysis. All animal experiments in this study followed the Principles of Laboratory Animal Care (NIH publication no. 85Y23; revised, 1996), and the experimental protocol was approved by the Animal Care Committee of Hebei University of Chinese Medicine Health Science Center.

2.3. Blood Analysis. Blood samples were collected from the orbital vein to measure baseline glucose levels after fasting for 14 h from mice. The mice were subjected to glucose (2 g/kg body weight) at 10 weeks on HFD or insulin (0.75 IU/kg body weight; Humulin) at 11 weeks on HFD by intraperitoneal injection. Blood samples were collected at 15, 30, 60, and 120 min (90 min for the insulin tolerance test) after glucose or insulin injection. An enzymatic kit (BioSino Bio-Technology and Science Inc., China) determined blood glucose levels. Blood samples were collected at 0, 4, 8, and 12 weeks of HFD for the determination of plasma total cholesterol (TC) and triacylglycerol (TG); TC, TG, LDL cholesterol (LDL-C), aspartate aminotransferase (AST), and alanine aminotransferase (ALT) were measured using an enzymatic kit (BioSino Bio-Technology and Science Inc., China). Insulin levels were determined using an ELISA kit (Excell, China). Blood samples for AST and ALT measurements were collected at the end of the HFD period. An enzymatic method was implemented to determine high-density lipoprotein cholesterol (HDL-C) levels, followed by precipitation of apolipoprotein B.

2.4. Histological Analysis. The hearts and livers were optimal cutting temperature (OCT) compound embedded and frozen at -20°C. The liver and aortic root sections were obtained by a continuous frozen section at a thickness of 7 μm. The sections were then fixed and stained with Oil Red

O, and lipid deposition was analyzed using ImageJ software. The liver and adipose tissues were embedded in paraffin, and 4- μ m tissue sections were obtained. The sections were stained using hematoxylin and eosin (HE) staining. ImageJ software was used to measure the area of the adipocytes ($n = 200$ adipocytes per animal and $n = 5$ animals per group).

2.5. RNA Isolation and Quantitative Real-Time PCR. Tissues were homogenized and extracted using TRIzol reagent (Invitrogen, Carlsbad, CA, USA). Chloroform extraction, isopropyl alcohol precipitation, and ethanol washing were performed, and total tissue RNA was obtained. First-strand cDNA was generated using an RT kit (Invitrogen). Quantitative real-time PCR (qRT-PCR) was performed using primers listed in Table 1. The comparative CT method was used for the relative quantitation of gene expression in the samples, which was normalized to GAPDH.

2.6. Western Blot Analysis. Radioimmunoprecipitation assay buffer was used to homogenize liver tissues, and the protein content was measured using a bicinchoninic acid protein assay kit (Pierce, Rockford, IL). Antibodies against *Akt*, phospho-*Akt* (Ser473) (Cell Signaling Technology, Danvers, MA, USA), CHOP, PDI, and β -actin (Proteintech, Wuhan, China) were used. ImageJ image analysis software was used to quantify and analyze protein bands. Arbitrary densitometry units were quantified and expressed as mean \pm SEM.

2.7. Lipid Deposition Analysis of Liver Tissues. Approximately 100 mg of liver tissues was homogenized in 1 mL of cold PBS. A mixture of chloroform and methanol (CHCl₃: CH₃OH = 2:1) was used for lipid extraction. Then, 1 mL 3% Triton X-100 was used to dissolve liver lipids after drying under nitrogen. The TG and TC levels were measured using the enzymatic methods described above.

2.8. Statistical Analysis. All data were represented as the mean (SEM). Statistical comparison between groups was carried out using a one-way ANOVA. A P value <0.05 was considered statistically significant. All analyses were performed using the GraphPad Prism software (GraphPad Software).

3. Results

3.1. Diet-Induced Hyperlipidemia Was Alleviated in the DHM-Treated LDLR^{-/-} Mice. A high-fat diet can induce metabolic disorders such as hyperlipidemia and insulin resistance. Therefore, we determined the plasma levels of TC and TG. As shown in Figure 1, hyperlipidemia was induced in the control group (HFD) compared to that in the normal control group (ND). In addition, plasma TC and TG levels were significantly lower in the DHM group (HFD + DHM) than those in the control group (Figures 1(a) and 1(b)). HDL-C, the major antiatherosclerotic lipoprotein, was measured. The results indicated that the plasma HDL-C level had increased. At the same time, LDL-C was significantly reduced in the DHM group compared to that in the control group (Figures 1(c) and 1(d)).

3.2. Diet-Induced Insulin Resistance Was Alleviated in the DHM-Treated LDLR^{-/-} Mice. Plasma glucose levels were measured to investigate the role of DHM in insulin resistance. Insulin resistance in mice was significantly aggravated in the HFD group compared to that in the ND group (Figure 2). No significant differences in plasma glucose levels were observed among the three groups (Figure 2(a)). However, glucose tolerance was remarkably improved in the DHM group compared to that in the control group (Figures 2(c) and 2(d)). Insulin tolerance test (ITT) and insulin levels were analyzed to determine the role of DHM in insulin sensitivity in HFD-fed mice. Results show that insulin levels decreased, and insulin sensitivity strikingly improved in the DHM group (Figures 2(b), 2(e), and 2(f)).

3.3. Diet-Induced Visceral Obesity Was Alleviated in the DHM-Treated LDLR^{-/-} Mice. HFD led to body weight gain and an increase in the adipose tissue (Figure 3). However, it did not significantly affect the food intake of mice compared to ND (data not shown). During 12 weeks of HFD, body weight was significantly reduced in the DHM group compared to that in the control group (Figure 3(a)). Moreover, visceral fat (such as retroperitoneal fat and epididymis fat) was significantly lower in the DHM group than that in the control group (Figure 3(b)). H&E staining and quantitative results of the adipocyte area of the two fat sections showed a slight decrease in adipocyte size in the DHM group compared to that in the control group (Figures 3(c)–3(f)). Further investigation by qPCR suggested that genes associated with lipid synthesis (*Scd1*) and lipid transport (*Mttp*) were downregulated, and genes related to fatty acid oxidation (*Acox1* and *Cpt1 α*) were upregulated in the DHM group compared to those in the control group (Figures 3(g) and 3(h)). In contrast, no significant differences were observed in lipolysis (*Atgl* and *Hsl*). Thus, our data demonstrated that DHM could decrease lipid synthesis, increase lipid catabolism, and prevent obesity in LDLR^{-/-} mice.

3.4. Diet-Induced Fatty Liver Was Alleviated in the DHM-Treated LDLR^{-/-} Mice. When the mice were treated with DHM, lipid levels were reduced (Figure 1). Elevated circulating lipid levels led to lipid deposition in the liver. Therefore, we assessed lipid deposition in the liver. Compared with the control group, the liver weight, TG, and TC contents were significantly lower in the DHM group mice (Figures 4(a)–4(c)). The decrease in liver lipid deposition was further confirmed by H&E and Oil Red O staining of liver tissue sections in the DHM group compared to that in the control group (Figure 4(d)). p-Akt, an insulin-sensitive organ, has been detected in the liver. A HFD significantly downregulated the expression of p-Akt, which was rescued by DHM (Figure 4(e)). Then, the expression of genes related to lipid metabolism was detected by qPCR. As shown in Figure 4(f), the mRNA levels of fatty acid oxidation (*Cpt1 α*), lipolysis (*Lpl*), and cholesterol ester transport (*Cetp*) were significantly upregulated, and this indicates that lipolysis and lipid transport increased in the DHM group.

TABLE 1: A list of primers for qPCR.

Gene	Forward	Reverse
<i>Gapdh</i>	TGATGACATCAAGAAGGTGGTGAAG	TCCTTGAGGCCATGTAGGCCAT
<i>Pparg</i>	GACCACTCGCATTCTTT	CCACAGACTCGGCACTCA
<i>Cetpa</i>	GTTAGCCATGTGGTAGGAGACA	CCCAGCCGTTAGTGAAGAGT
<i>Fasn</i>	GGTCTATGCCACGATTC	GTGTCCCATGTTGGATTG
<i>Acc1</i>	CTCCCGATTATAATTGGGTCTG	TCGACCTTGTTTACTAGGTGC
<i>Scd1</i>	CGCTGGCACATCAACTTCAC	AGGAACTCAGAAGCCCAAAGC
<i>Dgat2</i>	GCGTACTTCCGAGACTACTT	GGCCTTATGCCAGGAAACT
<i>Atgl</i>	ATGTTCCCAGGGAGACCAA	GAGGCTCCGTAGATGTGAGTG
<i>Hsl</i>	GATTTACGCACGATGACACAGT	ACCTGCAAAGACATTAGACAGC
<i>Cd36</i>	GGAGCCATCTTTGAGCCTTCA	GAACCAAAGTGGGAATGGATCT
<i>Ppara</i>	GGGCTTTCGGGATAGTTG	ATTGGGCTGTTGGCTGAT
<i>Pgc1a</i>	TATGGAGTGACATAGAGTGTGCT	GTCGCTACACCACTTCAATCC
<i>Acox1</i>	GTACCAGCGTCGGGGATTG	AAAGGCTCAGGATGCCCTCG
<i>Cpt1a</i>	CTCCGCCTGAGCCATGAAG	CACCAGTGATGATGCCATTCT
<i>Mttp</i>	ATACAAGCTCACGTACTIONACT	TCTCTGTTGACCCGCATTTTC

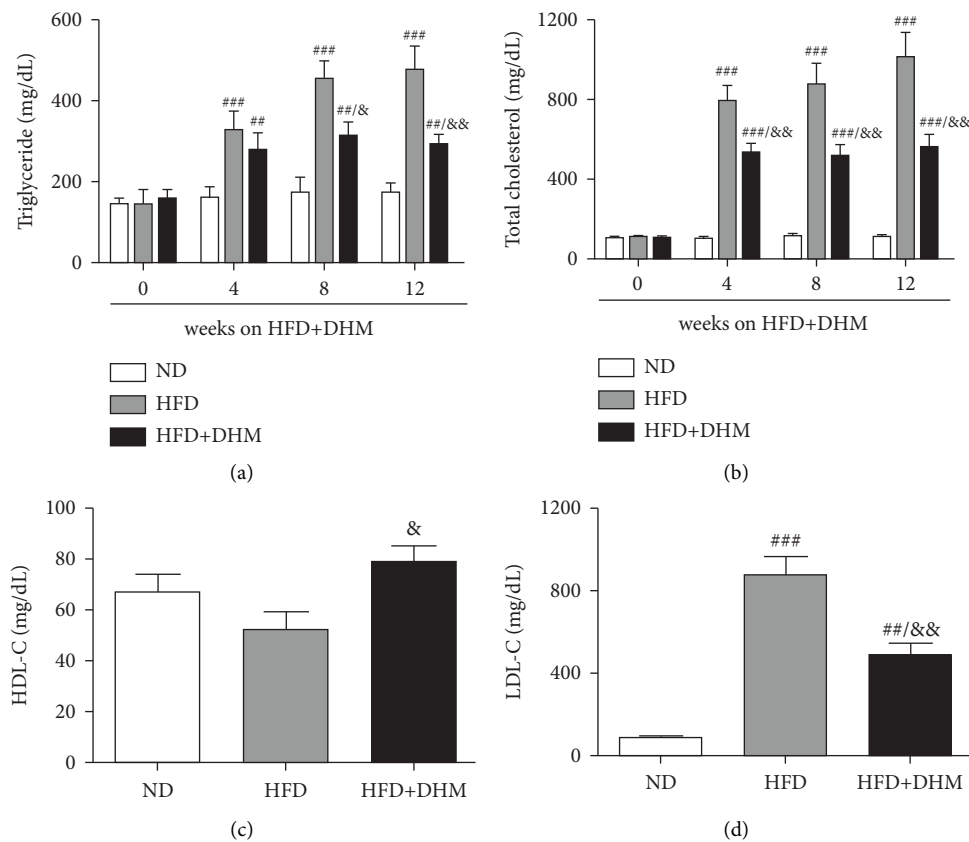


FIGURE 1: Diet-induced hyperlipidemia was alleviated in the DHM-treated $LDLR^{-/-}$ mice: (a, b) plasma total triglyceride and cholesterol levels before and during the DHM challenge and ND or HFD feeding, (c) plasma high-density lipoprotein cholesterol levels after eight weeks of the ND or HFD feeding, and (d) plasma low-density lipoprotein cholesterol levels after eight weeks of ND or HFD feeding, $n = 8$ per group; # compared with the normal control group (ND); &, compared with the control group (HFD); #/ & $p < 0.05$, ###/ && $p < 0.01$, and ### $p < 0.01$.

3.5. Diet-Induced Liver ER Stress Was Alleviated in the DHM-Treated $LDLR^{-/-}$ Mice. Liver function is influenced by lipid deposition. We then measured the plasma levels of aminotransferase. The results showed that the plasma levels of AST and ALT were significantly decreased when treated with

DHM compared to the control group (Figures 5(a) and 5(b)). ER stress in the liver was moderately alleviated, as detected by western blot analysis of CHOP (Figures 5(c) and 5(d)). Therefore, our data suggest that ER stress in the liver was moderately alleviated in the DHM group.

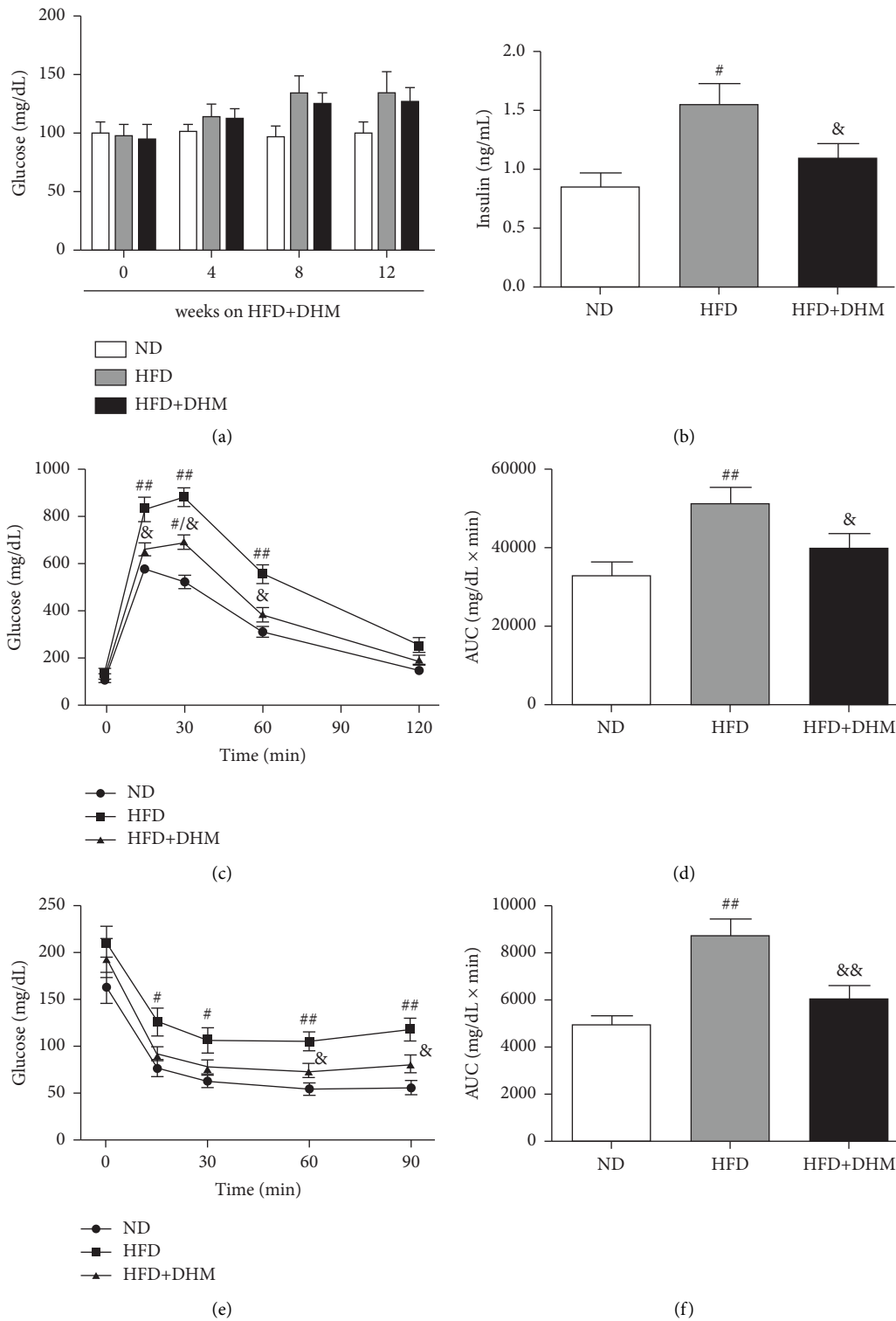
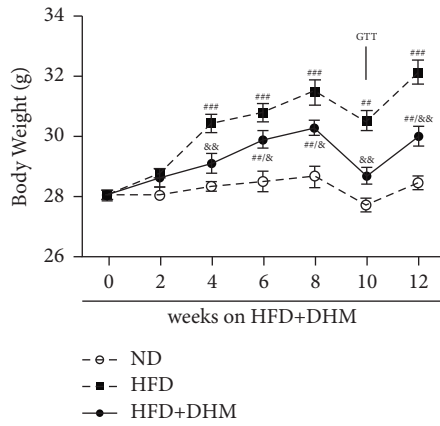
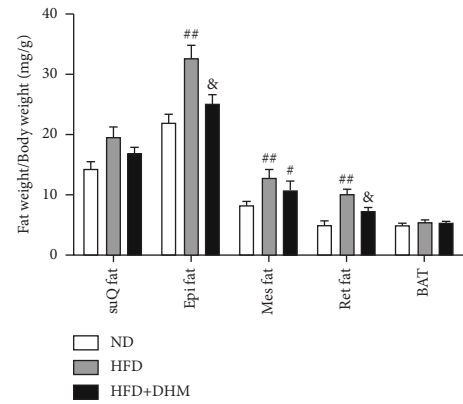


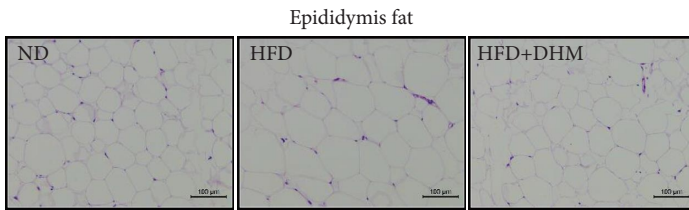
FIGURE 2: Diet-induced insulin resistance was alleviated in the DHM-treated LDLR^{-/-} mice: (a) plasma glucose levels before and during the DHM challenge and ND or HFD feeding, (b) plasma insulin levels after 12 weeks of ND or HFD feeding, (c) glucose tolerance test (GTT) after 10 weeks of ND or HFD feeding, (d) area under the curve shown in figure (C), (e) the insulin tolerance test (ITT) after 11 weeks of HFD, and (f) area under the curve of figure (E). *n* = 8 per group; # compared with the normal control group (ND); &, compared with the control group (HFD); #/& *P* < 0.05 and ##/&& *P* < 0.01.



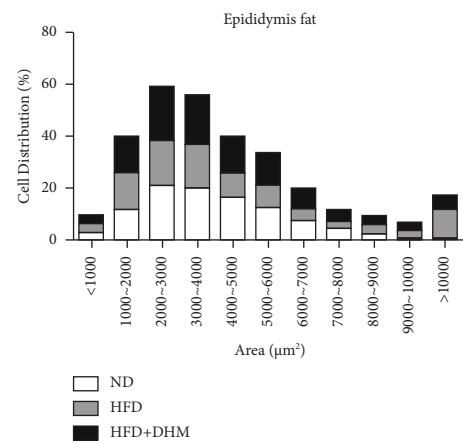
(a)



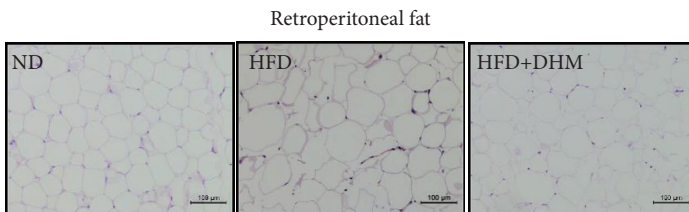
(b)



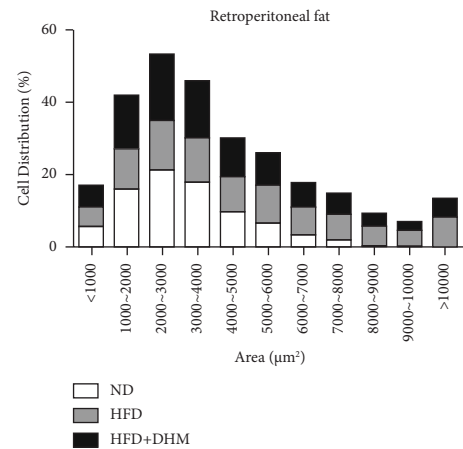
(c)



(d)



(e)



(f)

FIGURE 3: Continued.

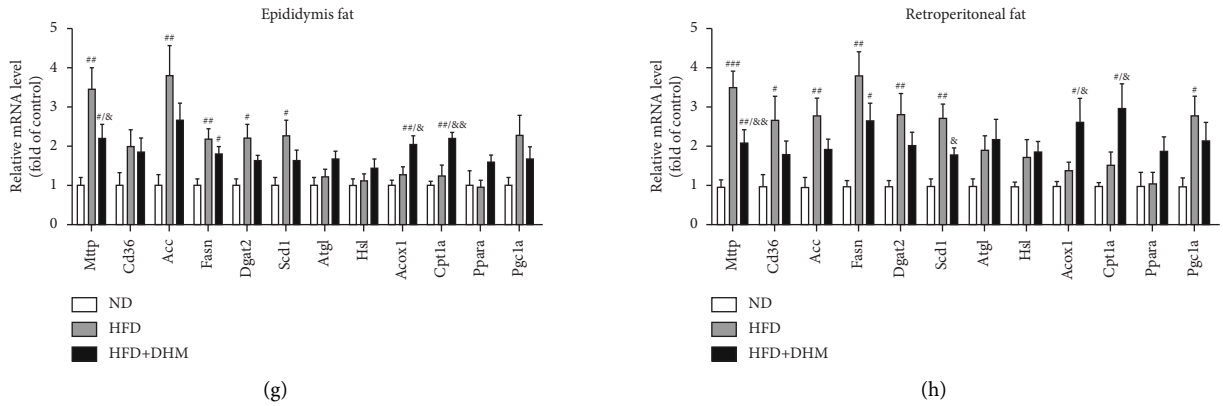


FIGURE 3: Visceral fat decrease in the DHM-treated LDLR^{-/-} mice: (a) body weight before and during the DHM challenge and ND or HFD feeding, (b) weight of adipose tissues; *n* = 8 per group and [#]*P* < 0.05, (c) hematoxylin and eosin (H&E) staining of epididymis fat; bar = 100 μm, (d) adipocyte size distribution in epididymis fat. ImageJ software was used for quantification. Distribution of adipocyte areas is shown in each column. Five mice with 200 adipocytes per mouse were analyzed for every distribution, (e) H&E staining of the retroperitoneal fat; bar = 100 μm, (f) adipocyte size distribution in retroperitoneal fat, (g) mRNA expression of genes in epididymis fat (*n* = 6 per group), and (h) mRNA expression of genes in the retroperitoneal fat (*n* = 6 per group). [#] Compared with the normal control group (ND); ^{#&} compared with the control group (HFD); ^{#/&} *P* < 0.05 and ^{##/&&} *P* < 0.01.

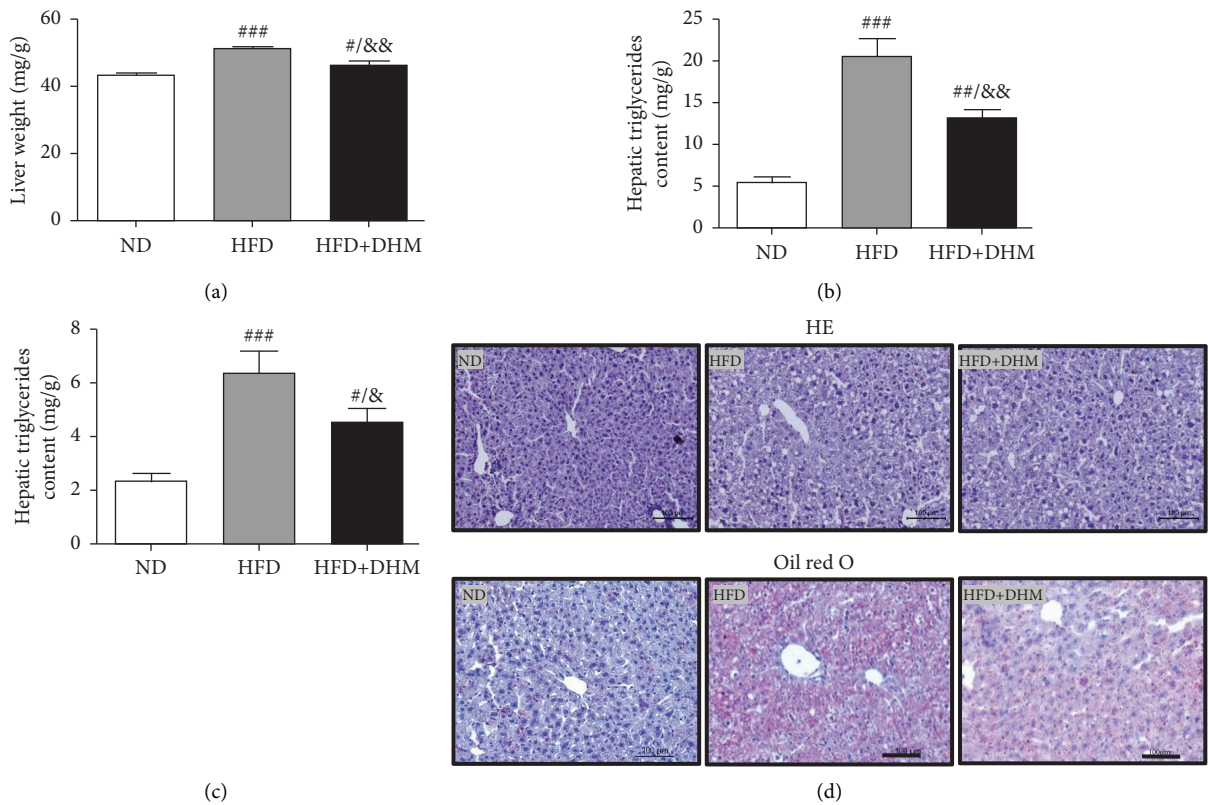


FIGURE 4: Continued.

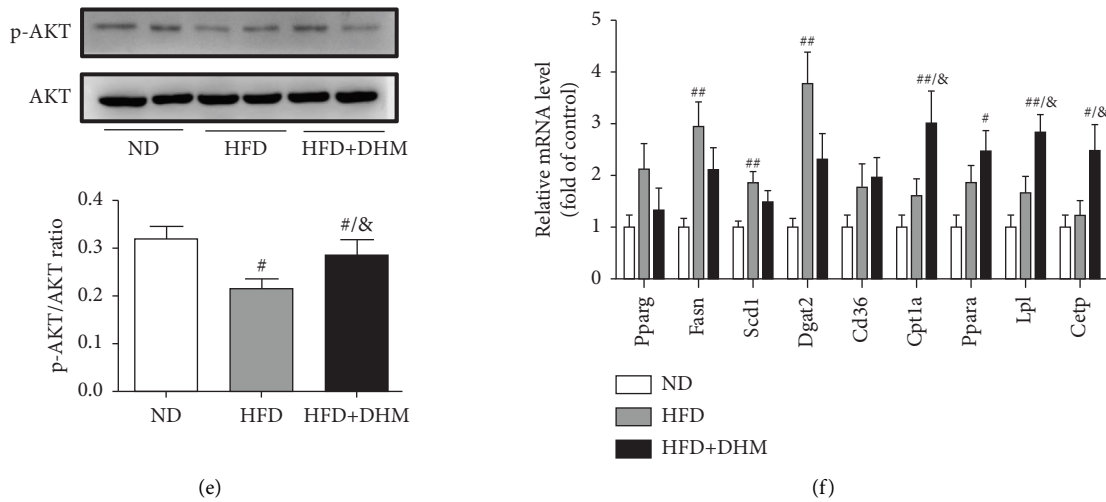


FIGURE 4: Diet-induced fat deposition was alleviated in the liver of the DHM-treated $LDLR^{-/-}$ mice: (a) liver weight, (b, c) total liver triglyceride and cholesterol content; $n = 8$ per group, (d) H&E (top) and Oil Red O (bottom) staining of the liver; bar = $100 \mu\text{m}$, (e) western blot analysis of p-Akt (Ser473) and total Akt in the liver ($n = 4$ per group), and (f) mRNA expression of genes related to triglyceride and cholesterol metabolism in the liver; $n = 6$ per group; [#]compared with the normal control group (ND); [&]compared with the control group (HFD); ^{#/&} $P < 0.05$, ^{##/&&} $P < 0.01$, and ^{###/&&&} $P < 0.001$.

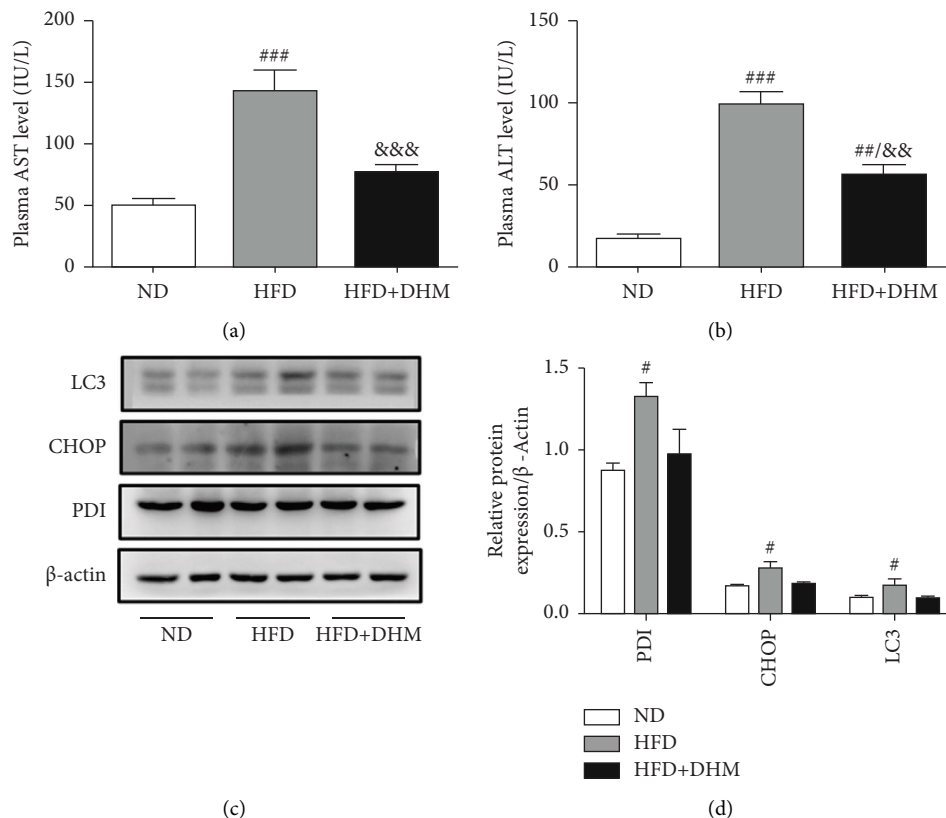


FIGURE 5: Diet-induced ER stress was alleviated in the liver of the DHM-treated $LDLR^{-/-}$ mice: (a, b) plasma AST and ALT levels after 12 weeks of high-fat diet (HFD) feeding, (c) western blot analysis of PDI, CHOP, and LC3 in the liver, (d) quantification of proteins shown in Figure (C); $n = 4$ per group; [#]compared with the normal control group (ND); [&]compared with the control group (HFD); ^{#/&} $P < 0.05$, ^{##/&&} $P < 0.01$, and ^{###/&&&} $P < 0.001$.

3.6. Diet-Induced Atherogenesis Was Alleviated in the DHM-Treated LDLR^{-/-} Mice. Atherogenesis could be aggravated in LDLR^{-/-} mice fed on HFD. Thus, we examined atherogenesis in the three groups of mice. A significant decrease in the As area, visualized by Oil Red O staining, was observed in the aortas of the DHM group after 12 weeks of HFD feeding (Figures 6(a) and 6(b)) and in the aortic root, compared with that in the aortas of the control group (Figures 6(c) and 6(d)). Moreover, the vessel and lumen areas in the aortic root were significantly increased in the DHM group (Figures 6(e) and 6(f)). These data suggest that DHM could alleviate atherogenesis and increase vessel and lumen areas.

4. Discussion

In this study, we explored the role of dihydromyricetin in NAFLD/NASH and its related insulin resistance, hyperlipidemia, and subsequent atherogenesis on HFD feeding in LDLR^{-/-} mice. Compared with the control group, we observed that (1) DHM significantly improved glucose tolerance and insulin sensitivity in mice; (2) the plasma levels of triglyceride, cholesterol, and visceral fat weight were significantly decreased; (3) liver lipid deposition was ameliorated, and liver cholesterol and triglyceride contents were significantly decreased; (4) liver function was dramatically improved, and ER stress was significantly suppressed; and (5) atherosclerotic lesions were significantly decreased in the DHM group.

The weights of retroperitoneal and epididymis fat in the DHM group decreased slightly (Figure 3). The down-regulated genes related to TG synthesis and lipid transport and reduced adipocytes size in retroperitoneal fat and epididymis fat suggested that DHM could reduce the expansion of visceral fat by promoting fat mobilization and the β -oxidation of fatty acids. NAFLD/NASH is typically characterized by the ectopic deposition of lipids in the liver, indicating an elevated liver TG content. In the DHM group, the liver TG content was significantly reduced, mainly due to enhanced oxidative metabolism, and this ultimately resulted in decreased lipid deposition in the liver (Figure 4). The expression of genes in the liver related to cholesterol reverse transport (*Cetp*) was upregulated, resulting in a moderate decrease of liver cholesterol content. *Akt* is a key downstream molecule of the insulin signaling pathway and plays an essential role in regulating glucose and lipid metabolism. *Akt* phosphorylation promotes glycogenesis and glycolysis [17]. Moreover, *Akt* regulates the sterol regulatory element-binding transcription factor (SREBP-1c) to influence lipogenesis [18]. DHM upregulated p-*Akt* levels in the liver, suggesting that insulin signaling was moderately activated in the DHM group. Moreover, *Akt* activation may affect cholesterol metabolism via SREBP-1c. These results suggest that DHM inhibits liver lipid deposition by promoting liver lipid oxidation and cholesterol metabolism.

Ectopic lipid deposition in the liver induces fatty liver with an increase in plasma total cholesterol, triglyceride, and LDL-C levels and affects the function of the liver, resulting in elevated plasma levels of AST, ALT, and bilirubin and a decrease in total protein and albumin [1]. Several studies

have shown that DHM plays a hepatoprotective role in mice fed with a high-fat diet, with reduced plasma lipid levels (such as TG, TC, and LDL-C) and transaminases of ALT or AST for instance [12, 19, 20]. In our study, the data showed that DHM reduce the plasma lipid levels and improve liver function, which is consistent with the results of previous studies.

Several studies have confirmed that a high-fructose diet can induce NASH and associated metabolic disorders [21]. Therefore, high-fructose diets are widely used in animal models of NASH and associated metabolic disorders. Unlike wild-type rodent animals, which hardly develop hyperlipidemia and As even though fed on a high-fat diet, LDLR^{-/-} mice are naturally prone to hypercholesteremia and As. They can develop hyperlipidemia and As when challenged with high-fat diet feeding, just like hypercholesteremic patients. Therefore, we investigated the role of DHM in NASH and related metabolic disorders induced by a high-fat and high-fructose diet in LDLR^{-/-} mice. Our results suggest that DHM could significantly alleviate insulin resistance induced by chronic HFD feeding, as confirmed by plasma insulin levels, GTT, and ITT. In addition, plasma lipid levels (measured using enzymic method) decreased. These results suggested that DHM can ameliorate NASH and associated hyperlipidemia, which is consistent with previous results.

The oral bioavailability of DHM is not high; however, it has obvious tissue distribution [22]. After oral administration, the concentration of DHM in the liver is approximately 20 times higher than that in the plasma [23, 24]. Thus, the amelioration of NAFLD by DHM may be related to DHM enrichment in the liver. Previous studies suggested that DHM could restrain NAFLD *in vivo* through several signaling pathways, such as NF κ B/ p53, SIRT3, and AMPK/ mTOR signaling and so on. However, the signaling pathway by which DHM alleviates NAFLD in LDLR^{-/-} mice fed on HFD was not explored in this study, which was the first limitation of our study.

The ER is an evolutionarily conserved organelle with a strong homeostatic system. However, many factors lead to an imbalance in ER homeostasis, resulting in ER stress. Stress caused by endoplasmic reperfusion injury, oxidative stress, and physicochemical damage can lead to excessive protein synthesis in cells that exceed the protein-folding capacity, resulting in ER calcium metabolism disorders, lecithin synthesis disorders, and ER stress [25]. Unfolded protein response reduces unfolded protein load under ER stress conditions. However, in situations where ER homeostasis is disrupted due to severe or prolonged stress or unusual challenges (such as energy or nutritional overload and inflammation), ER stress triggers responses that lead to cell death caused by apoptosis [26].

High circulating lipid and glucose levels increase ER stress. Dyslipidemia, NASH, and insulin resistance may result from dyslipidemia-dependent ER stress [27]. Several studies have confirmed that DHM can reduce ER stress in tumor tissues or cells through various pathways [15]. The liver, the main organ of metabolism, is important for maintaining metabolic homeostasis in the whole body. Therefore, the inhibition of ER stress in liver tissues is beneficial for alleviating NAFLD/NASH

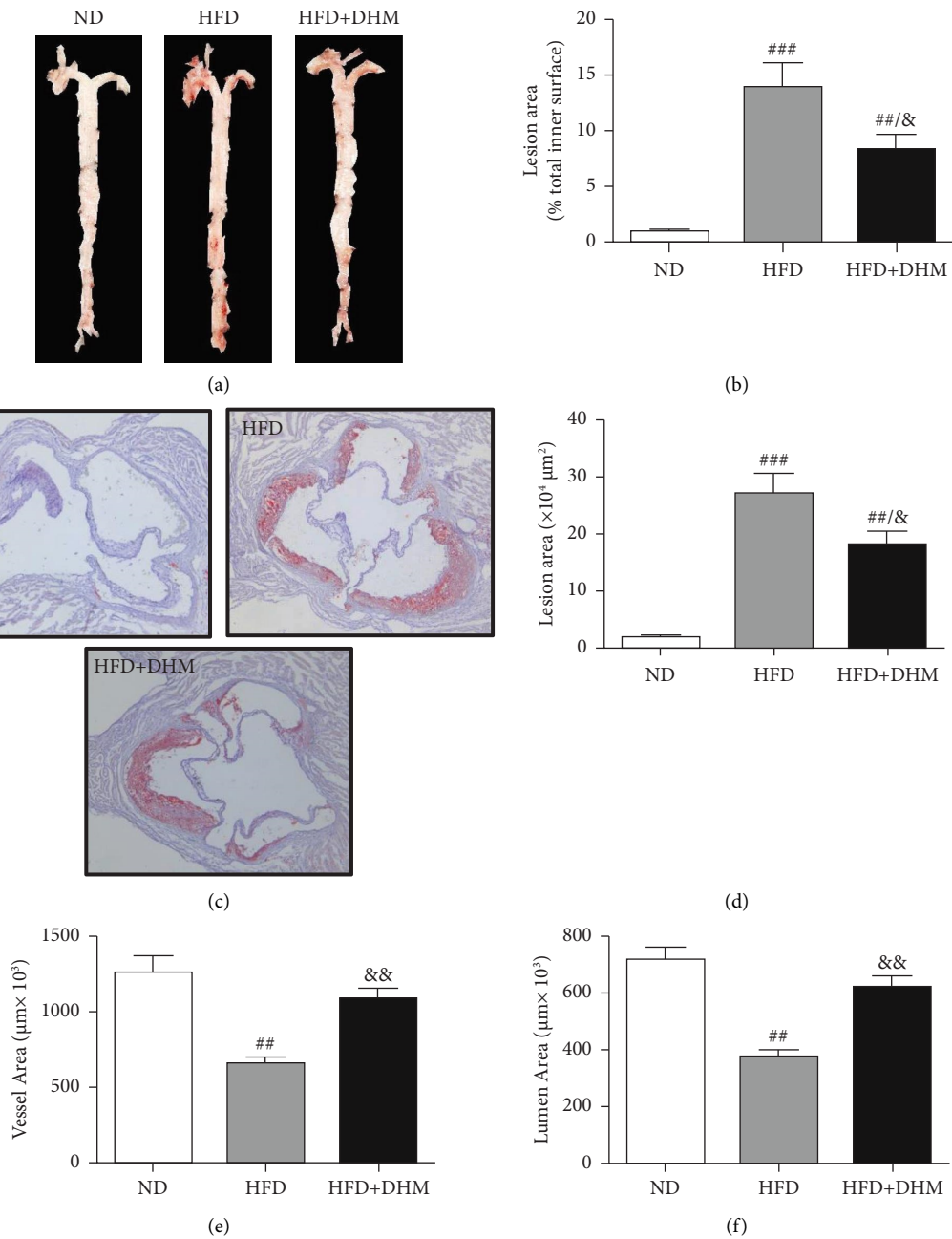


FIGURE 6: Atherosclerosis was alleviated in the DHM-treated LDLR^{-/-} mice: (a, b) Oil Red O staining of en face aorta and quantitative analysis of the aortic lesion area, (c, d) Oil Red O staining of the aortic root and quantitative analysis of the aortic root lesion area, (e) quantitative analysis of vessel areas in the aortic roots, and (f) quantitative analysis of the lumen area of aortic roots ($n = 8$ per group). # compared to the normal control group (ND); & compared with the control group (HFD); #/ & $P < 0.05$, ##/ & $P < 0.01$, and ### $P < 0.001$.

and related metabolic disorders [28]. Our results showed that DHM downregulated CHOP levels (Figure 5), suggesting that DHM could improve NASH by reducing ER stress in the liver. In eukaryotic cells, there are three ER stress response pathways: PKR-like eukaryotic initiation factor 2 α (eIF2 α) kinase (PERK), inositol-requiring enzyme 1 (IRE1), and activating transcription factor 6 (ATF6). CHOP is a vital molecule downstream of the PERK signaling pathway, and its downregulation indicates the amelioration ER stress in the liver. However, IRE1 α (an important UPR protein responsible for

the splicing of X-box binding protein1 for ER homeostasis) and ATF6 were not determined in this study which is the second limitation. Thus, further studies are required to confirm whether DHM influences these two proteins.

In DHM-treated mice, plasma HDL-C levels were elevated, which may be related to the decrease in the lesion area of As because HDL-C is antiatherosclerotic cholesterol. Moreover, DHM can interact with the gut microbiota to improve As [29]. Aortic remodeling plays a vital role in the repair of vascular injury and atherosclerosis [30]. However,

no studies have explored the effects of DHM on aortic remodeling. In our study, mice were subjected to HFD and DHM treatments to determine the role of DHM in preventing As aggravation and aortic remodeling. A reduction in the area of atherosclerotic lesions was observed in the mice treated with DHM. Moreover, the aortic root vessel and lumen areas were significantly enlarged compared to those in the control group, suggesting that DHM might promote aortic remodeling and increase effective blood flow. Plaque stability is closely associated with acute stroke and other cardiovascular and cerebrovascular diseases. Unstable plaques are characterized by more macrophages and foam cells, larger necrotic centers, and thinner fibrous caps. However, how DHM promotes vascular remodeling and whether DHM could improve plaque stability were not determined in this study and needed to be further explored, which is the third limitation of our study.

5. Conclusions

In conclusion, DHM, a compound isolated from many Chinese herbs, can improve NAFLD/NASH and related hyperlipidemia, adipogenesis, and insulin resistance by reducing ER stress in the liver, promoting vascular remodeling, and significantly preventing the formation of As.

Data Availability

The data used to support the findings of this study are available from L. L. and J. Z upon request.

Conflicts of Interest

The authors declare that they have no conflicts of interest.

Authors' Contributions

L. L. and J. Z. conceptualized the study; L. L., Q. S., H. L., and Y. W. performed data curation; L. L. and H. L. performed formal analysis; L. L. and J. Z. were responsible for funding acquisition; J. Z. investigated the data; L. L. and Y. W. contributed to methodology; J. Z. was involved in study supervision; L. L. prepared the original draft; Q. S., H. L., W. Y., and J. Z. reviewed and edited the manuscript; and Lin Liu, Quan Shen, Yan Wang, and Hong Li contributed equally to this work.

Acknowledgments

This research was funded by the Science and Technology Department of Hebei Province, 223777149D, and Natural Science Foundation of Hebei Province, H2020423061, to J. Z.; Science and Technology Project of Hebei Education Department, QN2022092, to L. L.; Hebei Traditional Chinese Medicine Administration, 2022080, to L. L. and, 2017009, to J. Z.; Medical Science Research Project of Hebei Provincial Health Commission, 20231564, to L. L.; and Dr. Fund of Hebei University of Chinese Medicine, BSZ2021007, to L. L.

References

- [1] J. C. Cohen, J. D. Horton, and H. H. Hobbs, "Human fatty liver disease: old questions and new insights," *Science*, vol. 332, no. 6037, pp. 1519–1523, 2011.
- [2] A. Wree, L. Broderick, A. Canbay, H. M. Hoffman, and A. E. Feldstein, "From NAFLD to NASH to cirrhosis-new insights into disease mechanisms," *Nature Reviews Gastroenterology & Hepatology*, vol. 10, no. 11, pp. 627–636, 2013.
- [3] L. V. Selby, A. Ejaz, S. A. Brethauer, and T. M. Pawlik, "Fatty liver disease and primary liver cancer: disease mechanisms, emerging therapies and the role of bariatric surgery," *Expert Opinion on Investigational Drugs*, vol. 29, no. 2, pp. 107–110, 2020.
- [4] J. Li, B. Zou, Y. H. Yeo et al., "Prevalence, incidence, and outcome of non-alcoholic fatty liver disease in Asia, 1999–2019: a systematic review and meta-analysis," *The Lancet Gastroenterology and Hepatology*, vol. 4, no. 5, pp. 389–398, 2019.
- [5] Z. M. Younossi, A. B. Koenig, D. Abdelatif, Y. Fazel, L. Henry, and M. Wymer, "Global epidemiology of nonalcoholic fatty liver disease-Meta-analytic assessment of prevalence, incidence, and outcomes," *Hepatology*, vol. 64, no. 1, pp. 73–84, 2016.
- [6] G. Targher, C. D. Byrne, and H. Tilg, "NAFLD and increased risk of cardiovascular disease: clinical associations, pathophysiological mechanisms and pharmacological implications," *Gut*, vol. 69, no. 9, pp. 1691–1705, 2020.
- [7] D. Cryer, "NASH and liver cancer: the new cancer headline," *American Journal of Managed Care*, vol. 25, no. 11, pp. P334–P335, 2019.
- [8] F. Scarpini, R. Cappellone, A. Auteri, and L. Puccetti, "Role of genetic factors in statins side-effects," *Cardiovascular and Haematological Disorders-Drug Targets*, vol. 12, no. 1, pp. 35–43, 2012.
- [9] M. Liu, H. Guo, Z. Li et al., "Molecular level insight into the benefit of myricetin and dihydromyricetin uptake in patients with alzheimer's diseases," *Frontiers in Aging Neuroscience*, vol. 12, Article ID 601603, 2020.
- [10] Q. Zhang, J. Liu, H. Duan, R. Li, W. Peng, and C. Wu, "Activation of Nrf2/HO-1 signaling: an important molecular mechanism of herbal medicine in the treatment of atherosclerosis via the protection of vascular endothelial cells from oxidative stress," *Journal of Advanced Research*, vol. 34, pp. 43–63, 2021.
- [11] L. Hou, F. Jiang, B. Huang et al., "Dihydromyricetin ameliorates inflammation-induced insulin resistance via phospholipase C-CaMKK-AMPK signal pathway," *Oxidative Medicine and Cellular Longevity*, vol. 2021, Article ID 8542809, 18 pages, 2021.
- [12] T. Liu, Y. Zeng, K. Tang, X. Chen, W. Zhang, and X. Xu, "Dihydromyricetin ameliorates atherosclerosis in LDL receptor deficient mice," *Journal of Vascular Surgery*, vol. 262, pp. 39–50, 2017.
- [13] L. Fan, X. Qu, T. Yi et al., "Metabolomics of the protective effect of Ampelopsis grossedentata and its major active compound dihydromyricetin on the liver of high-fat diet hamster," *Evidence-based Complementary and Alternative Medicine*, vol. 2020, Article ID 3472578, 15 pages, 2020.
- [14] J. He, J. Zhang, L. Dong et al., "Dihydromyricetin attenuates metabolic syndrome and improves insulin sensitivity by upregulating insulin receptor substrate-1 (Y612) tyrosine phosphorylation in db/db mice," *Diabetes, Metabolic*

- Syndrome and Obesity: Targets and Therapy*, vol. 12, pp. 2237–2249, 2019.
- [15] X. Kou, J. Fan, and N. Chen, “Potential molecular targets of ampelopsin in prevention and treatment of cancers,” *Anti-Cancer Agents in Medicinal Chemistry*, vol. 17, no. 12, pp. 1610–1616, 2017.
- [16] D. Yang, Z. Yang, L. Chen et al., “Dihydromyricetin increases endothelial nitric oxide production and inhibits atherosclerosis through microRNA-21 in apolipoprotein E-deficient mice,” *Journal of Cellular and Molecular Medicine*, vol. 24, no. 10, pp. 5911–5925, 2020.
- [17] H. V. Lin and D. Accili, “Hormonal regulation of hepatic glucose production in health and disease,” *Cell Metabolism*, vol. 14, no. 1, pp. 9–19, 2011.
- [18] J. D. Horton, J. L. Goldstein, and M. S. Brown, “SREBPs: activators of the complete program of cholesterol and fatty acid synthesis in the liver,” *Journal of Clinical Investigation*, vol. 109, no. 9, pp. 1125–1131, 2002.
- [19] Q. Lyu, L. Chen, S. Lin, H. Cao, and H. Teng, “A designed self-microemulsion delivery system for dihydromyricetin and its dietary intervention effect on high-fat-diet fed mice,” *Food Chemistry*, vol. 390, Article ID 132954, 2022.
- [20] J. Wu, K. Miyasaka, W. Yamada, S. Takeda, N. Shimizu, and H. Shimoda, “The anti-adiposity mechanisms of ampelopsin and vine tea extract in high fat diet and alcohol-induced fatty liver mouse models,” *Molecules*, vol. 27, no. 3, p. 607, 2022.
- [21] V. Svop Jensen, C. Fledelius, E. Max Wulff, J. Lykkesfeldt, and H. Hvid, “Temporal development of dyslipidemia and non-alcoholic fatty liver disease (NAFLD) in Syrian hamsters fed a high-fat, high-fructose, high-cholesterol diet,” *Nutrients*, vol. 13, no. 2, p. 604, 2021.
- [22] L. Liu, X. Yin, X. Wang, and X. Li, “Determination of dihydromyricetin in rat plasma by LC-MS/MS and its application to a pharmacokinetic study,” *Pharmaceutical Biotechnology*, vol. 55, no. 1, pp. 657–662, 2017.
- [23] Q. Tong, X. Hou, J. Fang et al., “Determination of dihydromyricetin in rat plasma by LC-MS/MS and its application to a pharmacokinetic study,” *Journal of Pharmaceutical and Biomedical Analysis*, vol. 114, pp. 455–461, 2015.
- [24] L. Fan, Q. Tong, W. Dong et al., “Tissue distribution, excretion, and metabolic profile of dihydromyricetin, a flavonoid from vine tea (*Ampelopsis grossedentata*) after oral administration in rats,” *Journal of Agricultural and Food Chemistry*, vol. 65, no. 23, pp. 4597–4604, 2017.
- [25] P. Walter and D. Ron, “The unfolded protein response: from stress pathway to homeostatic regulation,” *Science*, vol. 334, no. 6059, pp. 1081–1086, 2011.
- [26] C. M. Scull and I. Tabas, “Mechanisms of ER stress-induced apoptosis in atherosclerosis,” *Arteriosclerosis, Thrombosis, and Vascular Biology*, vol. 31, no. 12, pp. 2792–2797, 2011.
- [27] E. Burgos-Morón, Z. Abad-Jiménez, A. M. Marañón et al., “Relationship between oxidative stress, ER stress, and inflammation in type 2 diabetes: the battle continues,” *Journal of Clinical Medicine*, vol. 8, no. 9, p. 1385, 2019.
- [28] M. Parafati, R. J. Kirby, S. Khorasanizadeh, F. Rastinejad, and S. Malany, “A nonalcoholic fatty liver disease model in human induced pluripotent stem cell-derived hepatocytes, created by endoplasmic reticulum stress-induced steatosis,” *Disease Models & Mechanisms*, vol. 11, no. 9, Article ID dmm033530, 2018.
- [29] L. Fan, X. Zhao, Q. Tong et al., “Interactions of dihydromyricetin, a flavonoid from vine tea (*Ampelopsis grossedentata*) with gut microbiota,” *Journal of Food Science*, vol. 83, no. 5, pp. 1444–1453, 2018.
- [30] D. Kapetanios, R. Banafsche, T. Jerkku et al., “Current evidence on aortic remodeling after endovascular repair,” *The Journal of Cardiovascular Surgery*, vol. 60, no. 2, pp. 186–190, 2019.